PCCP

COMMUNICATION

Cite this: *Phys. Chem. Chem. Phys.*, 2019, **21**, 12763

Received 7th May 2019,
Accepted 3rd June 2019

DOI: 10.1039/c9cp02538c

rsc.li/pccp

Threshold photoelectron spectrum of the CH_2OO Criegee intermediate†

David V. Chicharro, [a] Sonia Marggi Poullain, [b] Luis Bañares, *[a] Helgi Rafn Hrodmarsson, [c] Gustavo A. García *[c] and Jean-Christophe Loison *[d]

We present the photoelectron spectroscopy of the simplest Criegee intermediate, CH_2OO, close to the first ionization energy. Comparison with existing theoretical data yields the experimental adiabatic ionization energy and provides a benchmark for theoretical studies on larger Criegee intermediates, which play an important role in the ozonolysis of alkenes.

Carbonyl oxides were postulated by Criegee in the 1950s to be formed in the ozonolysis of alkenes[1] as intermediates in a three-step mechanism that is now generally accepted.[2] The detection and study of carbonyl oxides, also known as Criegee intermediates (CIs), are of considerable atmospheric importance considering that alkenes are the second largest anthropogenic and biogenic organic volatiles after methane.[3] Additionally, ozonolysis is an important mechanism for their atmospheric removal, as well as an important pathway to OH formation in winter and night-time. CIs enhance the oxidizing capacity of the atmosphere *via* different chemical pathways by undergoing unimolecular reactions leading to OH formation,[4,5] or reacting with water, SO_2, NO_2, *etc.* Tangentially, reactions with other organic molecules such as acids or carbonyls lead to other oxidized organics that eventually evolve into secondary organic aerosols, thus enhancing aerosol formation.[6] The interested reader will find a more exhaustive review on the reactivity of carbonyl oxides elsewhere.[7,8]

Although there is a large amount of literature on CIs, the first direct detection was not achieved until 2008,[9] where the simplest CI, CH_2OO, was identified in a gas phase reactor by photoionization mass spectrometry and its formaldehyde oxide structure was confirmed over all other possible isomers by comparing the experimental photoionization efficiency (PIE) curve at m/z 46 to the calculated one.[10] The gas phase structure was later corroborated by infrared spectroscopy.[11] Therein, the CH_2OO bond lengths were found to be more comparable with those of a zwitterion rather than a biradical, as already suggested in the pioneering photoionization study. The first direct measurement of its reactivity followed four years later, where the rate constant for the oxidation of SO_2 to SO_3 by CH_2OO was obtained and found to be much larger than originally predicted. This highlights the importance of these challenging experiments.[12] Recently, the CH_2OO intermediate has been directly observed in the gas phase in the ozonolysis of ethylene by microwave spectroscopy.[13]

In spite of the accumulating experimental data on this intermediate, its adiabatic ionization energy is not precisely known. Experiments gave a first estimation of this value at $\sim$9.96 eV,[9] while theoretical calculations have provided values ranging from 9.931 to 10.02 eV.[9,10,14,15] In this work, we have recorded for the first time the photoelectron spectrum of CH_2OO close to the first adiabatic ionization energy, yielding an accurate value for the adiabatic ionization energy. Comparison of this value, along with the simulated photoelectron spectrum, provides a more stringent test of the model than the existing PIE curves, which is critical to confidently move towards modelling larger CIs.

Additionally, in the last decade, the mass tagged photoelectron spectrum obtained through photoelectron photoion coincidence (PEPICO) techniques[16] has been used as a fingerprint for multiplex species identification in complex media, since the obtained vibronic structure provides more specificity and sensitivity than PIE curves, which is advantageous specially when isomer differentiation is necessary.[17–20]

Experiments have been performed at the DESIRS beamline of the French synchrotron SOLEIL,[21] on the permanent endstation SAPHIRS.[22] The continuous microwave (MW) discharge flow-tube reactor used in the present experiments has been

[a] *Departamento de Química Física, Facultad de Ciencias Químicas, Universidad Complutense de Madrid, 28040 Madrid, Spain*
[b] *Departamento de Química, Módulo 13, Facultad de Ciencias, Universidad Autónoma de Madrid, 28049 Madrid, Spain*
[c] *Synchrotron SOLEIL, L'Orme des Merisiers, St. Aubin, BP 48, 91192 Gif sur Yvette, France. E-mail: garcia@synchrotron-soleil.fr*
[d] *ISM, Université Bordeaux 1, CNRS, 351 cours de la Libération, 33405 Talence Cedex, France*

† Electronic supplementary information (ESI) available: Experimental methodology, TOFMS recorded at $h\nu$ = 12.0 eV, comparison between experimental and theoretical PIEs, comparison between experimental and calculated photoelectron spectra at the B3LYP/6-311++G** and M06-2X/aug-cc-pVTZ levels of theory. See DOI: 10.1039/c9cp02538c

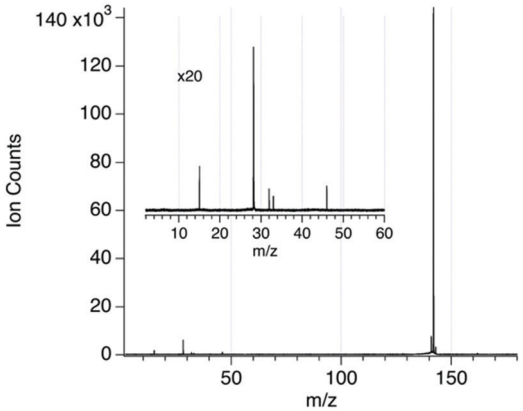

Fig. 1 Time-of-flight mass spectrum (TOFMS) obtained by integrating all mass spectra for photon energies from 9.8 to 10.4 eV. The inset shows a zoom on the region corresponding to the lighter masses.

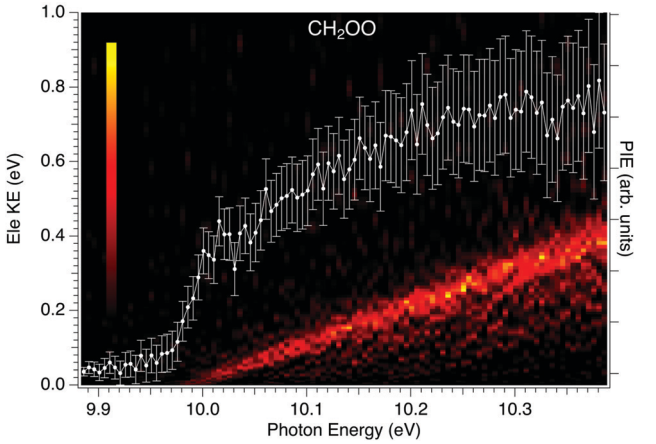

Fig. 2 Intensity colormap representing the electron signal as a function of electron kinetic energy (eleKE) and photon energy for the *m*/*z* 46 channel. The white curve with error bars corresponds to the photoionization efficiency (PIE) as a function of photon energy.

described in detail elsewhere[23] and the relevant parameters are discussed at length in the ESI.† Briefly, CH_2OO is formed by reaction between CH_2I and O_2, where the iodomethyl radical is produced by H abstraction from the iodomethane precursor:

$$F_2 \xrightarrow{MW} 2F$$

$$CH_3I + F \rightarrow CH_2I + HF$$

The chemical species produced in the reactor are ionized by the synchrotron VUV radiation and the electrons and ions are detected in coincidence using a double imaging PEPICO (i^2PEPICO) device.[24]

Fig. 1 shows the time-of-flight mass spectrum (TOFMS) accumulated over the photon energy range 9.8–10.4 eV. Apart from the peak of interest at *m*/*z* 46 corresponding to CH_2OO, the mass channels *m*/*z* 15, 28, 32, 33, 141, 142 and 143 are also visible and assigned *via* their vibronic structure to the CH_3 radical, metastable $N_2(A\ ^3\Sigma_u^+)$, O_2 (traces from the remaining second order ionization), CH_2F and CH_2I radicals, CH_3I and $^{13}CH_3I$, respectively.

There are several possible channels for the reaction between CH_2I and O_2: production of CH_2OO + I, production of the CH_2IOO adduct and a minor channel leading to formation of formaldehyde and IO. As in previous photoionization mass spectrometry (PIMS) experiments,[9,12,25] the CH_2IOO channel is not observed since we would expect stabilisation of this species to occur only at high reactor pressures, although it could also be that the parent ion is not stable within the energy range of this work. TOFMS data obtained over the ionization energy (IE) of formaldehyde, at $h\nu$ = 12 eV (see Fig. S1 of the ESI†), shows a small signal at *m*/*z* 30 that could correspond to formaldehyde, although its low signal-to-noise precludes an unambiguous identification. Additionally, the counterpart product, IO, is not seen in the *m*/*z* 143 channel. Only a vibronic structure consistent with $^{13}CH_3I$ is detected in that channel and the ratio between the areas of the *m*/*z* 143 and *m*/*z* 142 peaks corresponds to the expected natural abundance of the ^{13}C isotope within our error bars. We do see atomic iodine in Fig. S1 (ESI†), alongside HI, I_2 and IF.

Fig. 2 shows the electron signal as a function of the electron kinetic energy and photon energy for the *m*/*z* 46 channel. Energy conservation leads to diagonal lines of constant unity slope (constant ionic state, CIS, lines) for each cationic state *i*: eKE/($h\nu$ − IE_i), where eKE is the electron kinetic energy and IE_i is the ionization energy of the *i*th state. From this matrix, several relevant projections can be plotted, such as the well-known PIE curve obtained by integrating over all the electron energies, which is also depicted in Fig. 2 and Fig. S2 of the ESI.† The curve is in agreement with previous experiments.[9,12]

However, as indicated above, integration greatly reduces the spectroscopic information contained in the curve. Hence other projections such as the photoelectron spectrum (PES) at a given photon energy, or the threshold photoelectron spectrum (TPES) are more desirable. The latter is obtained by integrating the signal along the CIS lines over only the slowest photoelectrons ($\mathrm{TPES}(h\nu) = \int_0^{\delta(\mathrm{eKE})} I(h\nu + x, x)\mathrm{d}x$, where δ(eKE) = 20 meV, and $I(h\nu$,eKE) is the coincident signal intensity as a function of photon and electron energy, as depicted in Fig. 2), so that only transitions between neutral and cationic states that are resonant with the photon energy will appear.[26] The TPES for the *m*/*z* 46 channel is depicted in Fig. 3, and shows a main feature centered at 9.99 eV. Both the PIE and the TPES show that the only isomer present in the reactor is the CH_2OO since the other possible isomers (formic acid, dioxirane, ethanol and dimethyl ether) have very different ionization energies and/or vibronic structure. For instance, dimethyl ether has a similar ionization energy (10.025 eV), but its TPES is different,[27] and the production route used in this work is known to yield CH_2OO quite efficiently, while generation of CH_3OCH_3 is very unlikely.

Nguyen *et al.*[10] calculated that the singlet ground state of the neutral formaldehyde oxide could be better defined as having zwitterion character based on the bond lengths and the

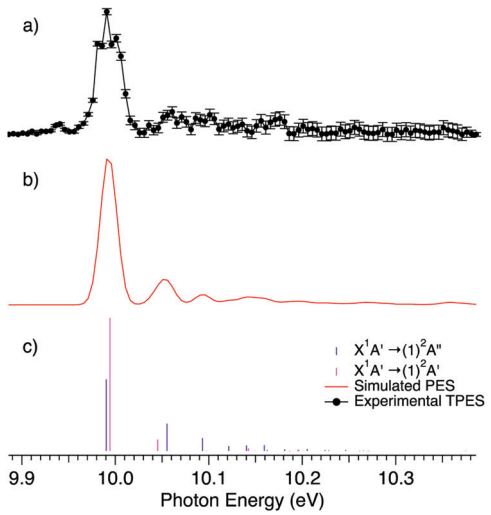

Fig. 3 (a) Experimental threshold photoelectron spectrum (TPES), (b) simulated PES and (c) calculated Franck–Condon (FC) factors at the QCISD/6-31G** level of theory from Lee *et al.*[14] The simulated PES and calculated FC factors have been shifted by 20 meV from the calculated adiabatic ionization energy. The energy scale is accurate to within ±3 meV (see ESI†).

configuration interaction wave function. The same authors also calculated the first adiabatic ionization energy at the CCSD(T)–CBS level and found a value of 9.98 eV for the $(1)^2A' \leftarrow \tilde{X}^1A'$ transition, that corresponds mainly to the removal of the electron from the terminal oxygen atom. The accuracy of the calculated adiabatic ionization energy (IE_{ad}) was estimated at 50 meV, mostly due to zero-point energy errors. The authors placed the first neutral triplet state at 1.8 eV above the $^1A'$ ground state, but we have not detected ionization transitions from this state, most likely because the internal energy of the nascent CH_2OO is lower, the $CH_2I + O_2 \rightarrow CH_2OO + I$ being only slightly exothermic, between 50 and 130 meV.[12,14] Taatjes *et al.* performed a Franck–Condon (FC) harmonic simulation using optimized CBS-QB3 geometries[7] and found an intense adiabatic transition due to the small geometry change between the neutral $\tilde{X}^1A'$ ground state and the cationic $(1)^2A'$ ground state, which agrees with our experimental spectrum shown in Fig. 3a.

In a more complete theoretical work, Lee *et al.*[14] calculated ionization transitions to the cationic ground and first excited states, $(1)^2A'$ and $(1)^2A''$, using a large variety of theoretical methods. These states are very close in energy, so it is not yet conclusive which of them is the ''actual'' ground state. The calculated adiabatic energies at their highest level of theory for transitions to the A′ and A″ states are 9.974 eV and 9.971 eV, respectively. Lee *et al.* simulated the photoelectron spectrum using a harmonic model and an equal weighting for the A′ and A″ transitions. At the QCISD/6-31G** level of theory, an intense adiabatic peak was obtained with weak excitation in the COO bending and O–O stretching modes, mainly in the A″ state, as shown in Fig. 3c.

The agreement between the simulated spectrum in Fig. 3b, obtained by convolving the stick spectrum with a Gaussian having a full-width-half-maximum (FWHM) of 20 meV, and the experimental spectrum of Fig. 3a is remarkably good, including the higher energy vibrational structure seen between 10.02 and 10.2 eV, although the experimental signal-to-noise ratio combined with the weak FC factors is not sufficient to provide reliable vibrational frequencies. A small feature at 9.94 eV, which does not correspond to the IE_{ad} of any of the aforementioned isomers, is seen in the spectrum and could correspond to a hot band that would be consistent with excitation of one quantum of the COO bending mode in the neutral, calculated by Lee *et al.* at around 500 cm^{-1}. In Fig. S3 of the ESI† we show the comparison between experiment and the simulated spectrum obtained by Lee *et al.* at the B3LYP/6-311++G** level of theory, where we find a somewhat worse qualitative agreement.

Note that for both simulations, the best agreement between simulated and experimental spectra is obtained by shifting the calculated IE_{ad} by 20 meV, from 9.971 eV to 9.991 eV. This provides an experimental IE_{ad} value of 9.991 ± 0.005 eV, where the error bar takes into account the precision of the energy scale and the inability to distinguish between the A′ and A″ states. This value leads to an enthalpy of formation of the cation of $\Delta H_f(0\ K)(CH_2OO^+)$ = 1076.3 ± 0.8 kJ mol^{-1}, using the recommended ATcT[28] enthalpy of formation for CH_2OO, 112.43 ± 0.61 kJ mol^{-1}.

More recent calculations by Huang *et al.* at the DLPNO-CCSD(T)/aug-cc-pVXZ (X = T, Q) level of theory[15] suggest a larger separation of the A′ and A″ transitions, of 70 meV instead of 3 meV. Although their simulated PIE curve reportedly matches the existing experimental ones, and as shown in Fig. S2 (ESI†), the PIE obtained in this work, the simulated PES shown in Fig. S4 of the ESI† does not agree with our experimental spectrum. Perhaps an explanation for the disagreement can be found in the systematic theoretical study of the CH_2OO CI, where Lee *et al.*[14] observed that the ordering and energy differences of the A′ and A″ transitions, as well as the FC factors, were very sensitive to the level of theory. In any case, within the measured 18 meV experimental resolution we do not see two separate adiabatic transitions, which supports the Lee *et al.* findings and disagrees with the predictions of Huang *et al.*

In conclusion, the present study reports an accurate measurement of the adiabatic ionization energy (IE_{ad}) of the simplest CI, CH_2OO. Our measured threshold photoelectron spectrum is consistent with the calculations by Lee *et al.*[14] but disagrees with the more recent calculations by Huang *et al.*[15] While both calculations seem to provide good agreement with existing PIE curves, the simulated photoelectron spectrum is shown to be very sensitive to the level of theory. Therefore, the experimental TPES reported here provides a more rigorous benchmark of the calculations in order to move towards larger CIs. Finally, the spectrum depicted in Fig. 3 not only validates the theoretical methods, but can also serve as a precise fingerprint for the identification of these elusive species in atmospheric or combustion reactions using photoelectron photoion coincidence techniques.[29]

Conflicts of interest

There are no conflicts to declare.

Acknowledgements

This work was performed at the DESIRS beamline. We acknowledge SOLEIL for provision of synchrotron radiation facilities under proposal number 20180727, and the DESIRS beamline staff for their assistance. S. M. P. acknowledges financial support for a postdoctoral contract (PEJD-2016/IND-3217) from the Regional Government of Madrid (Spain) through the European Social Fund and the Fondo de Garantía Juvenil. D. V. C. acknowledges a contract from Spanish MINECO under the FPI predoctoral program. Financial support from Spanish MINECO through grants CTQ2015-65033-P and PGC2018-09644-B-I00 is gratefully acknowledged. This work received financial support from the French Agence Nationale de la Recherche (ANR) under grant ANR-12-BS08-0020-02 (project SYNCHROKIN).

Notes and references

1 R. Criegee and G. Wenner, *Justus Liebigs Ann. Chem.*, 1949, **564**, 9.
2 R. Criegee, *Angew. Chem., Int. Ed. Engl.*, 1975, **14**, 745.
3 A. H. Goldstein and I. E. Galbally, *Environ. Sci. Technol.*, 2007, **41**, 1514.
4 A. Novelli, L. Vereecken, J. Lelieveld and H. Harder, *Phys. Chem. Chem. Phys.*, 2014, **16**, 19941.
5 M. I. Lester and S. J. Klippenstein, *Acc. Chem. Res.*, 2018, **51**, 978.
6 W. Ahmad, C. Coeur, A. Cuisset, P. Coddeville and A. Tomas, *J. Aerosol Sci.*, 2017, **110**, 70.
7 C. A. Taatjes, *Annu. Rev. Phys. Chem.*, 2017, **68**, 183.
8 P. O. Wennberg, K. H. Bates, J. D. Crounse, L. G. Dodson, R. C. McVay, L. A. Mertens, T. B. Nguyen, E. Praske, R. H. Schwantes, M. D. Smarte, J. M. St Clair, A. P. Teng, X. Zhang and J. H. Seinfeld, *Chem. Rev.*, 2018, **118**, 3337.
9 C. A. Taatjes, G. Meloni, T. M. Selby, A. J. Trevitt, D. L. Osborn, C. J. Percival and D. E. Shallcross, *J. Am. Chem. Soc.*, 2008, **130**, 11883.
10 M. T. Nguyen, T. L. Nguyen, V. T. Ngan and H. M. T. Nguyen, *Chem. Phys. Lett.*, 2007, **448**, 183.
11 Y.-T. Su, Y.-H. Huang, H. A. Witek and Y.-P. Lee, *Science*, 2013, **340**, 174.
12 O. Welz, J. D. Savee, D. L. Osborn, S. S. Vasu, C. J. Percival, D. E. Shallcross and C. A. Taatjes, *Science*, 2012, **335**, 204.
13 C. C. Womack, M. A. Martin-Drumel, G. G. Brown, R. W. Field and M. C. McCarthy, *Sci. Adv.*, 2015, **1**, e1400105.
14 E. P. F. Lee, D. K. W. Mok, D. E. Shallcross, C. J. Percival, D. L. Osborn, C. A. Taatjes and J. M. Dyke, *Chem. – Eur. J.*, 2012, **18**, 12411.
15 C. Huang, B. Yang and F. Zhang, *J. Chem. Phys.*, 2019, **150**, 164305.
16 J. H. D. Eland, *Int. J. Mass Spectrom. Ion Phys.*, 1972, **8**, 143.
17 A. Bodi, P. Hemberger, D. L. Osborn and B. Sztaray, *J. Phys. Chem. Lett.*, 2013, **4**, 2948.
18 P. Oßwald, P. Hemberger, T. Bierkandt, E. Akyildiz, M. Köhler, A. Bodi, T. Gerber and T. Kasper, *Rev. Sci. Instrum.*, 2014, **85**, 025101.
19 B. Cunha de Miranda, G. A. Garcia, F. Gaie-Levrel, A. Mahjoub, T. Gautier, B. Fleury, L. Nahon, P. Pernot and N. Carrasco, *J. Phys. Chem. A*, 2016, **120**, 6529.
20 J. Pieper, S. Schmitt, C. Hemken, E. Davies, J. Wullenkord, A. Brockhinke, J. Krüger, G. A. Garcia, L. Nahon, A. Lucassen, W. Eisfeld and K. Kohse-Höinghaus, *Z. Phys. Chem.*, 2018, **232**, 153.
21 L. Nahon, N. de Oliveira, G. A. Garcia, J.-F. Gil, B. Pilette, O. Marcouillé, B. Lagarde and F. Polack, *J. Synchrotron Radiat.*, 2012, **19**, 508.
22 X. Tang, G. A. Garcia, J.-F. Gil and L. Nahon, *Rev. Sci. Instrum.*, 2015, **86**, 123108.
23 G. A. Garcia, X. Tang, J.-F. Gil, L. Nahon, M. Ward, S. Batut, C. Fittschen, C. A. Taatjes, D. L. Osborn and J.-C. Loison, *J. Chem. Phys.*, 2015, **142**, 164201.
24 G. A. Garcia, B. K. C. de Miranda, M. Tia, S. Daly and L. Nahon, *Rev. Sci. Instrum.*, 2013, **84**, 053112.
25 A. J. Eskola, D. Wojcik-Pastuszka, E. Ratajczak and R. S. Timonen, *Phys. Chem. Chem. Phys.*, 2006, **8**, 1416.
26 J. C. Poully, J. P. Schermann, N. Nieuwjaer, F. Lecomte, G. Gregoire, C. Desfrançois, G. A. Garcia, L. Nahon, D. Nandi, L. Poisson and M. Hochlaf, *Phys. Chem. Chem. Phys.*, 2010, **12**, 3566.
27 J. J. Butler, D. M. P. Holland, A. C. Parr and R. Stockbauer, *Int. J. Mass Spectrom. Ion Processes*, 1984, **58**, 1.
28 B. Ruscic and D. H. Bross, Active Thermochemical Tables (ATcT) values based on ver. 1.122 of the Thermochemical Network (2016); available at https://atct.anl.gov (accessed 8th of March 2019).
29 T. Baer and R. P. Tuckett, *Phys. Chem. Chem. Phys.*, 2017, **19**, 9698.

